Springer

KSME

Journal of Mechanical Science and Technology 26 (2) (2012) 427~436
www.springerlink.com/content/1738-494x
DOI 10.1007/s12206-011-1030-7

An optimal design for axial-flow fan blade: theoretical and experimental studies †

Cheng-Hung Huang* and Chung-Wei Gau

Department of Systems and Naval Mechantronic Engineering, National Cheng Kung University, Tainan, Taiwan, R.O.C

(Manuscript Received December 8, 2010; Revised September 11, 2011; Accepted September 27, 2011)

Abstract

The technique of inverse design problem (IDP) for optimizing the three-dimensional shape of an axial-flow fan blade based on the desired airflow rate is presented in this work. The desired volume flow rate of air can be obtained from the airflow rate of the existing axial-flow fan by multiplying it with a constant which is greater than unity. The geometry of the redesigned fan blade is generated using numerous design variables, which enables the shape of the fan blade to be constructed completely; thus the technique of parameter estimation for the inverse design problem can be used in this study. Results show that with the redesigned optimal fan blade, the airflow rate of fan can be increased, thereby improving the performance of the axial-flow fan. Finally, to verify the validity of this work, the prototypes of the original and optimal axial-flow fan blades are fabricated and fan performance tests are conducted with these blades on the basis of the AMCA-210-99 standard. The algorithm used in the present study can be applied to the blade design problem in any propulsion and power systems.

Keywords: Axial-flow fan; Fan blade design; Levenber-Marquardt method; Optimal design

1. Introduction

Fans, due to their reliable and simple structures, are adopted widely in various industrial applications, such as in HVAC, computers, automobiles, ships and electronic appliance units. Additionally, different types of fans are applied depending on the specified purpose. Axial-flow fans are normally used when a higher air flow rate in the system is required. Generally, axial-flow fans can be used for cooling small electronic devices such as home appliances and personal computers.

Because of the various applications of axial-flow fans, the fan blade design problem becomes an important issue to the fan makers. They have to develop their own design technology efficiently. The analysis (or direct) problem needs be done repeatedly in the traditional design algorithms by modifying the design variables, so it depends strongly on the designer's skills and experiences and requires much trial and error time to obtain the good design of the fan blades [1, 2].

In contrast to the traditional designing methods, the inverse design method provides an efficient algorithm to design an optimum blade shape that meets the operational conditions and specified constraints with minimum efforts [3-5], i.e., the time used for design modifications can be reduced. The direct fan blade problems are concerned with the determination of the air velocity, pressure and fan efficiency when the operational conditions, system parameters and the shape of fan blade are all specified. In contrast, the inverse design problem for axial-flow fan blade considered in this paper involves the determination of the optimal shape of fan blade for the axial-flow fan based on the desired airflow rate of fan.

Numerous studies regarding this topic can be found in the open literature. Lin et al. [6] applied an integrated approach combining the artificial neural network, the optimization algorithm, computational fluid dynamics and the machining method to design an optimal three-dimensional blade for an axial-flow fan. Seo et al. [7] considered an optimum fan blade design problem to design the blade stacking line for an axial-flow fan with response surface method and evaluated the effects of sweep and lean on the performance of the fan blade. Lee et al. [8] presented a numerical optimization procedure in determining the optimum fan blades for a low-speed axial-flow fan with polynomial response surface approximation model. Recently Lee et al. [9] used the inverse design code TURBOdesign-1to design the axial-flow fans for cooling condensers.

A general purpose commercial code, CFD-ACE+, released by ESI-CFD Inc. [10], is adopted in the present work as the solver for three-dimensional Reynolds-averaged Navier-Stokes equations with standard k-ε turbulence model. The

† This paper was recommended for publication in revised form by Associate Editor Byeong Rog Shin

* Corresponding author. Tel.: +886 6 2747018, Fax.: +886 6 2747019
E-mail address: chhuang@mail.ncku.edu.tw

advantage of calling CFD code as a subroutine in this fan blade design problem lies in its characteristics of easily-handling the moving grid problem considered here since it has the function of automatic grid generation.

An important first step in the proper formulation of the problem is to identify design variables for the blade. If proper variables are not selected, the formulation will be either incorrect or not possible at all. At the initial stage of the problem formulation, all possible design variables should be investigated. Sometimes it is desirable to designate more design variables than may be apparent from the problem in the initial stage; later, it is possible to assign a fixed numerical value to any variable and thus eliminate it from the problem formulation [11].

A four-digit-NACA airfoil NACA-mpta is used as the initial design for fan blade and the design variables are chosen as blade section parameters; for the case of NACA4609, the blade section parameters are 4 (m), 6 (p) and 09 (ta) three variables, setting angle (θ), twist angle (ϕ), blade root chord (Lr), blade end chord (Le), upper hub height (H_u) and lower hub height (H_l), respectively. The computation time for this blade design problem depends strongly on the number of design variables, so design variables should be selected appropriately. Essentially, design variables that have a strong effect on the fan performance should be selected. For this reason, the sensitivity analysis of these design variables must be examined to determine the critical design variables for use in the present inverse design problem.

The Levenberg-Marquardt method [12] has proven to be a powerful algorithm in inverse design calculations. This inverse design method had been applied to predict the form of a ship's hull in accordance with the desired hull pressure distribution by Huang et al. [13]. Subsequently, Chen and Huang [14] applied it to predict an unknown hull form based on the preferable wake distribution in the propeller disk plane. Chen et al. [15] further applied it to the aspect of optimal design for a bulbous bow. Moreover, Huang and Chen [16] and Huang and Lin [17] applied the similar technique to design the shape of gas channel for a proton exchange membrane fuel cell.

For this reason, the Levenberg-Marquardt algorithm is adopted in this paper to address the development of an efficient method for parameter estimation in estimating the optimal fan blade geometry that satisfies the desired (or optimal) airflow rate of fan. Finally, experiments are conducted based on the original and optimal fan blades to examine the discrepancy between the numerical and experimental results.

2. The direct problem

For the numerical simulation model, a fan is located at the flow passage to drive the air and the fluid flow is assumed to be steady, incompressible, and three-dimensional. The three-dimensional governing equations of continuity and momentum in the steady turbulent main flow using the standard k–ε model are shown in Eqs. (1) to (5), respectively [18, 19]:

$$\frac{\partial \rho \overline{u}_i}{\partial x_i} = 0 , \tag{1}$$

$$\rho \overline{u}_j \frac{\partial \overline{u}_i}{\partial x_j} = -\frac{\partial \overline{p}}{\partial x_i} + \frac{\partial}{\partial x_j}[\mu_t (\frac{\partial \overline{u}_i}{\partial x_j} + \frac{\partial \overline{u}_j}{\partial x_i})] , \tag{2}$$

$$\rho \overline{u}_j \frac{\partial k}{\partial x_j} = \frac{\partial}{\partial x_j}(\frac{\mu_t}{\sigma_k}\frac{\partial k}{\partial x_j}) + \mu_t (\frac{\partial \overline{u}_i}{\partial x_j} + \frac{\partial \overline{u}_j}{\partial x_i})\frac{\partial \overline{u}_i}{\partial x_j} - \rho\varepsilon , \tag{3}$$

$$\rho \overline{u}_j \frac{\partial \varepsilon}{\partial x_j} = \frac{\partial}{\partial x_j}(\frac{\mu_t}{\sigma_\varepsilon}\frac{\partial \varepsilon}{\partial x_j}) + C_1 \mu_t \frac{\varepsilon}{k}(\frac{\partial \overline{u}_i}{\partial x_j} + \frac{\partial \overline{u}_j}{\partial x_i})\frac{\partial \overline{u}_i}{\partial x_j} - C_2 \rho \frac{\varepsilon^2}{k} . \tag{4}$$

Since the Navier–Stokes equations are solved inside the duct domain, the no-slip boundary condition is applied to all the walls in the domain. Therefore, at all of the surfaces $\overline{u}_i = 0$.

In this study, all the above continuity and momentum equations in the steady turbulent flow using the standard k–ε model are solved by a general purpose computational fluid dynamic code, employing a finite volume method, since it has the ability to handle this moving grids problem using the "GRID DEFORMATION" function embedded in it. The "moving grids problem" actually implies that the grids along the blade edge can be fitted well with the grids in the flow field when the blades are rotating. The boundary type of the model inlet was set with velocity-inlet and turbulence intensity.

The outlet type was set with pressure-outlet. The constructive computational grid system is built by commercial code CFD-ACE+.

In addition, the coupled set of equations needs be solved iteratively, and the solution is considered to be convergent when the relative error in flow field between two consecutive iterations is less than a specified small number. Finally, the volume flow rate of the specific fan with known shape of blades can be obtained.

3. Shape generation for fan blade

The following nine design variables can be adopted to generalize the shape of fan blade: blade section parameters, m, p, ta (for the case of a four-digit-NACA airfoil NACA-mpta, the blade section parameters are namely m, p and ta three variables), setting angle (θ), twist angle (ϕ), blade root chord (Lr), blade end chord (Le), upper hub height (H_u) and lower hub height (H_l). The cross-sectional view of the NACA fan blade is shown in Fig. 1(a), while Fig. 1(b) indicates the design variables of the fan blade.

The shape generating procedure for fan blade can be summarized as follows: First, by applying the formula for a four-digit-NACA airfoil, the cross-sectional data for the blade can be obtained and saved in a specified type file name. This file is imported into CFD code, together with the information of blade root chord and blade end chord; the shape of untwisted blade can be obtained by using the embedded function in CFD code. By assigning the setting angle, twist angle, hub diameter

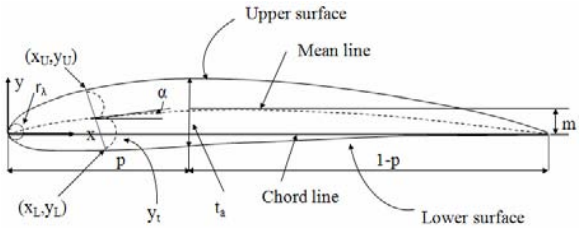

(a)

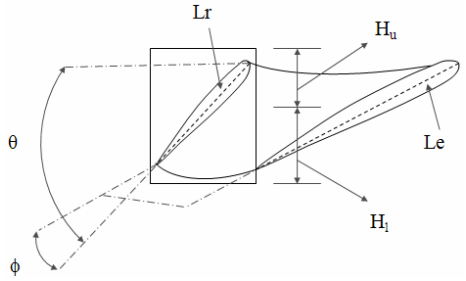

(b)

Fig. 1.The (a) geometric parameters of a two-dimensional NACA blade section; (b) design variables of the rotor blade.

and hub height, a single blade can be mounted on the hub, and finally the rest of blades can be duplicated by executing the rotate function in CFD code to obtain a complete fan blade.

The preceding blade geometry generation process can be saved in a python type file name. To obtain the new complete fan blades, one needs just input the above nine design variables and run the python file. This simple fan blade generation process makes the fan blade design problem neat and efficient.

4. The shape design problem

The objective function for optimal design of an axial flow fan blade is commonly chosen as the fan efficiency. However, the reason for not choosing it as our cost function in this study is because that higher fan efficiency does not guarantee higher air flow rate of fan. For some high heat intensity producing applications, the system needs to be cooled down at any cost to prevent overheating. The only objective function that can be chosen for such applications becomes the fan air flow rate.

For the shape design problem or inverse geometry design problem considered here, the shape of the redesigned fan blade is regarded as being unknown and is controlled by a set of design variables; in addition, the desired volume flow rate of air for fan is considered available.

Let the design variables and desired volume flow rate of air be denoted by B_j and Θ, respectively; the inverse geometry design problem can then be stated as follows: utilizing the above mentioned desired volume flow rate of air, Θ, design the new shape for the fan blade, Ψ . It should be noted that the desired volume flow rate of air, Θ, is always at static pressure equal to zero: Ps = 0.

The solution of the present inverse geometry design problem is to be obtained in such a way that the following functional is minimized:

$$J[\Psi(B_j)] = \{Q[\Psi(B_j)] - \Theta\}^2 = U^T U \ ; \ \ j = 1 \text{ to } P \ . \qquad (5)$$

Here, B_j, j = 1 to P, represent design variables, i.e.,

$$\begin{aligned} B_j = \mathbf{B} &= \{B_1, B_2, B_3, B_4, B_5, B_6, B_7, B_8, B_9\} \\ &= \{ m, p, ta, \theta, \phi, Lr, Le, H_u, H_l\} \end{aligned} \qquad (6)$$

and $Q[\Psi(B_j)]$ represents the estimated or computed volume flow rate of air at Ps =0. This quantity is determined from the solution of the direct problem given previously by using an estimated fan blade $\Psi(B_j)$, with design variables B_j. If the estimated volume flow rate of air Q is close enough to the desired volume flow rate of air Θ, the corresponding estimated fan blade $\Psi(B_j)$ can be regarded as the optimal shape of the redesigned fan blade.

When it requires that the perpendicular lengths of the chords for entire blade are the same, i.e., the sweep volume of blade is the same for all chords, the following constraint is needed:

$$Lr \times \sin\theta = Le \times \sin\phi \ . \qquad (7)$$

For this reason the design variable ϕ can be omitted here since it can be calculated from other three variables. Therefore, the variables used for the sensitivity analysis are taken as follows:

$$\begin{aligned} \mathbf{B} &= \{B_1, B_2, B_3, B_4, B_5, B_6, B_7, B_8\} \\ &= \{ m, p, ta, \theta, Lr, Le, H_u, H_l\}. \end{aligned} \qquad (8)$$

As was mentioned before, the identification of proper design variables for the fan blade is an important step in the present design problem. In the initial stage of design it is desirable to designate more design variables than may be apparent from the problem; later, it is possible to assign a fixed numerical value to any variable and thus eliminate it from the problem formulation. For this purpose the following sensitivity analysis for the design variables will be done to select only the effective design variables to reduce the computer time in the design process.

The influences of the design variables on the air volume flow rate are determined by perturbing the design variables B_j one at a time by $\pm 5\%$ of the original value (for m, p and ta, used ± 1) and computing the resulting changes in volume flow rate of air from Eqs. (1) to (4), i.e., the solution of the direct problem. If the changes in airflow rate are small for some design variables, these design variables are not sensitive to the design and can be set as fixed variables in the designing process.

5. The Levenberg-Marquardt method (LMM) for minimization

The next step in the analysis is the minimization of the least squares Eq. (5) by differentiating it with respect to each of the

unknown design variables. If P design variables are used, Eq. (5) is minimized with respect to the design variables B_j and then setting the resulting expression equal to zero. We thus found

$$\frac{\partial J[\Psi(B_j)]}{\partial B_j} = \{\frac{\partial Q[\Psi(B_j)]}{\partial B_j}\}[Q-\Theta]= 0 \ ; \ \ j = 1 \text{ to } P \ . \quad (9)$$

Eq. (9) is linearized by expanding $Q[\Psi(B_j)$ in Taylor series and retaining the first-order terms. Then a damping parameter μ^n is added to the resulting expression to improve convergence. This will finally lead to the Levenberg-Marquardt method [12] and is given by

$$(\mathbf{F} + \mu^n \mathrm{I})\Delta\mathbf{B} = \mathbf{D} \quad (10)$$

where

$$\mathbf{F} = \vartheta^T \vartheta \ , \quad (11)$$

$$\mathbf{D} = \vartheta^T \mathbf{U}, \quad (12)$$

$$\Delta\mathbf{B} = \mathbf{B}^{n+1} - \mathbf{B}^n \quad (13)$$

where the superscripts n and T represent the iteration index and transpose matrix, respectively, $\mathbf{I}$ is the identity matrix, and ϑ denotes the Jacobian matrix defined as

$$\vartheta = \frac{\partial Q}{\partial \mathbf{B}^T} \ . \quad (14)$$

The Jacobian matrix defined by Eq. (14) is determined by perturbing the unknown parameters B_j one at a time and computing the resulting change in volume flow rate of air from the solution of the direct problem.

Eq. (10) is now written in a form suitable for iterative calculation as

$$\mathbf{B}^{n+1} = \mathbf{B}^n + (\vartheta^T \vartheta + \mu^n \mathrm{I})^{-1} \vartheta^T (Q - \Theta) \ . \quad (15)$$

When $\mu^n = 0$, Newton's method is obtained, as $\mu^n \to \infty$, the steepest-descent method is obtained. For fast convergence the steepest-descent method is applied first, then the value of μ^n is decreased; finally, Newton's method is used to obtain the inverse solution. The algorithm of choosing this damping value μ^n is described in detail by Marquardt [12].

The bridge between CFD code and LMM is the INPUT/OUTPUT files. The information from CFD code to LMM is the calculated volume flow rate of air and the Jacobian matrix, and the information from LMM to CFD code is the new estimated shape for the fan blade. These files should be arranged such that their format can be recognized by both CFD code and LMM. A sequence of forward fan blade problems is solved by CFD code in an effort to update the fan blade geometry by minimizing a residual measuring the difference between estimated and desired volume flow rate of air under the present algorithm.

When the airflow rate is obtained the following equation can be used to calculate the efficiency of fan blade

$$\eta = \frac{Ps \times Q}{\tau \times \omega} \quad (16)$$

where Ps represents static pressure, τ is the torque of blade, and ω denotes fan speed.

6. Computation procedure

The iterative computational procedure for the solution of this inverse design problem using the Levenberg-Marquardt method can be summarized as follows.

Choose an existing fan blade to start the computations; the design variables at the zeroth iteration, B_j^0, can be obtained from this blade and are used as the starting reference variables. The desired volume flow rate of air Θ is also given in the very beginning.

Step 1. Solve the direct problem by using CFD code to obtain the estimated or computed volume flow rate of air, $Q[\Psi(B_j)]$.

Step 2. Check the stopping criterion; if not satisfied go to Step 3.

Step 3. Construct the Jacobian matrix in accordance with Eq (14).

Step 4. Update **B** from Eq. (15), and compute the new fan blade in accordance with the standard procedure stated in section 3. Go to Step 1 and iterate.

7. The statistical analysis

Statistical analysis is important in determining the reliability of the estimated design variables. In this section the confidence bounds analysis is developed for the estimated design variables, **B**, by assuming independent, constant-variance errors. The variance-covariance matrix of the estimated design variables vector **B** is defined as [20]

$$\text{Var-cov}(\mathrm{B}) \equiv E[\mathbf{B} - E(\mathbf{B})][\mathbf{B} - E(\mathbf{B})]^T \quad (17)$$

where $\mathbf{B} = \mathbf{B}(\Theta)$ is the unknown design variables vector, Θ is the desired volume flow rate of air, $E(\bullet)$ denotes the statistical expected value (averaging) operator, and superscript T refers to the transpose. Eq. (17) is a nonlinear system for the determination of the variance-covariance matrix

The right hand side of Eq. (17) is then linearized by expanding **B** and E(**B**) in Taylor series and neglecting the higher-order terms. We thus obtain

$$\text{Var-cov}(\mathbf{B}) = \left[\frac{\partial \mathbf{B}}{\partial \Theta^T}\right] E\left[\ [\Theta - E(\Theta)][\Theta - E(\Theta)]^T\ \right] \left[\frac{\partial \mathbf{B}^T}{\partial \Theta}\right] . \quad (18)$$

For independent volume flow rate measurements with constant variance σ^2, we have [20]

$$E[[\Theta - E(\Theta)][\Theta - E(\Theta)]^T] = \sigma^2 \mathbf{I} . \quad (19)$$

Introducing Eq. (19) into Eq. (18), the variance-covariance matrix becomes

$$\text{Var-cov}(\mathbf{B}) = \sigma^2 \left[\frac{\partial \mathbf{B}}{\partial \Theta^T} \right] \left[\frac{\partial \mathbf{B}^T}{\partial \Theta} \right] . \quad (20)$$

To express the right-hand side of Eq. (20) in terms of Jacobian, the chain-rule is applied and the high-order terms are neglected. After some length manipulations the following equation is obtained:

$$\text{Var-cov}(\mathbf{B}) = \sigma^2 \left\{ \left[\frac{\partial \mathrm{Q}^{\mathrm{T}}}{\partial \mathbf{B}} \right] \left[\frac{\partial \mathrm{Q}}{\partial \mathbf{B}^{\mathrm{T}}} \right] \right\}^{-1} . \quad (21)$$

Here, the Jacobian matrix and its transpose are evaluated from the results of direct problem by perturbing the unknown parameters.

If we assume independent errors, the nondiagonal elements in the variance-covariance matrix vanish and can be written in explicit form as

$$\text{Var-cov}(\mathbf{B}) = \begin{bmatrix} \sigma^2_{\mathrm{B_1}} & 0 & \cdots & 0 \\ 0 & \sigma^2_{\mathrm{B_2}} & & \vdots \\ \vdots & & \ddots & 0 \\ 0 & \cdots & 0 & \sigma^2_{\mathrm{B_P}} \end{bmatrix} . \quad (22)$$

Then a comparison of Eqs. (21) and (22) gives the standard deviation of the estimated parameters $\sigma_{\mathbf{B}}$ as

$$\sigma_{\mathbf{B}} = \sigma \sqrt{\text{diag} \left\{ \left[\frac{\partial \mathrm{Q}^{\mathrm{T}}}{\partial \mathbf{B}} \right] \left[\frac{\partial \mathrm{Q}}{\partial \mathbf{B}^{\mathrm{T}}} \right] \right\}^{-1}} \quad (23)$$

where σ is the standard deviation of the measurements for the air flow rate. This result is identical to the one given by Maniatty and Zabaras [21]. Based on Eq. (23), if the measurement error is assumed normal distribution, it is quite intuitive that the estimates are normal as well.

Once the standard derivation of the estimated design variables is obtained, it is natural that some confidence bounds are of interest. For this reason Flach and Ozisik [22] proposed the equation of the confidence bounds for the estimated quantities.

If we now assume a normal distribution for the measurement errors, the 99% confidence bounds are determined as [22]

$$\{\mathbf{B} - 2.576\sigma_{\mathbf{B}} \le \mathbf{B}_{mean} \le \mathbf{B} + 2.576\sigma_{\mathbf{B}}\} = 99\% . \quad (24)$$

Table 1. The system variables for various fan blades considered in this work.

	Original fan blade	Optimal fan blade	Designed fan blade #1	Designed fan blade #2
NACA airfoil (mpta)	4609	5608	4506	4609
Blade root chord (Lr, mm)	18.0	19.38	17.59	18.17
Blade end chord (Le, mm)	33.0	37.86	30.64	34.18
Setting angle (θ,°)	47	59	33.18	52.22
Number of blades	7	7	7	7
Fan speed (ω, rpm)	2500	2500	2500	2500
Hub diameter (D_{Hub}, mm)	40.0	40.0	40.0	40.0
Fan diameter (D, mm)	110.0	110.0	110.0	110.0
Hub height (H_u+H_l=H, mm)	15.0	15.0	15.0	15.0
Fan gap (mm)	2.0	2.0	2.0	2.0
Air volume flow rate (Q, CFM)	78.19	88.84	63.0	83.0

This expression defines the approximate statistical confidence bounds for the estimated design variables vector **B**, i.e., the estimated values of design variables are expected to lie between these two bounds with 99% confidence.

8. Experiments for fan blade performance testing

A fan performance test was conducted with the original and optimal fan blades on the basis of the AMCA-210-99 standard. This standard defines uniform methods for conducting laboratory tests on house fans to determine airflow rate, pressure, power and efficiency at a given speed of rotation. The duct on the experiment is an outlet-side test duct of category B, and pitot tubes (united sensor) were used as the pressure sensor. The air volume flow rate was measured using the Yokogawa WT1600 power meter with an accuracy rating of ±0.1%.

The purpose of the experiments is to test the accuracy of CFD code, i.e., to show that the numerical and experimental airflow rates for fan blades are consistent under the specified operational and geometrical conditions. The measurement of torque of blade is difficult in a fan blade experiment, so we substituted the calculated numerical value of torque into the fan efficiency equation, together with the measured air flow rate, static pressure and rotating frequency of fan blade, to calculate the experimental fan efficiency.

9. Results and discussion

The system variables for the original fan blade are shown in Table 1 and the shape of the fan blade can be constructed in accordance with the technique stated in section 3, SHAPE GENERATION FOR FAN BLADE, and the grid system for the fan blades and computational domain can be obtained automatically by using CFD code. Fig. 2(a) shows the computational domain of the fan-duct system considered here. After the fan blade grid systems are obtained, the volume flow rate of air can be calculated using CFD code.

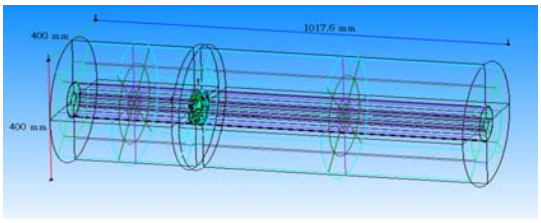

(a)

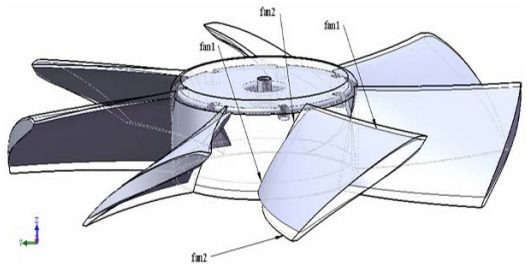

fan 1: Original fan,
fan 2: Optimal fan

(b)

Fig. 2. The (a) computational domain of fan-duct system; (b) a comparison of the original and optimal fan blades.

Table 2. Sensitivity analysis for the design variables.

Variable	Perturbed condition	Resultant CFM	Percentage change in CFM
θ=47.0°	49.35° (+5%)	79.94	+2.23%
θ=47.0°	44.65° (–5%)	76.39	–2.30%
Le=33.0 mm	34.65 mm (+5%)	79.26	+1.36%
Le=33.0 mm	31.35 mm (–5%)	77.11	–1.39%
Lr=18.0 mm	18.90 mm (+5%)	79.93	+2.22%
Lr=18.0 mm	17.10 mm (–5%)	76.48	–2.19%
H_u=5.0 mm	5.25 mm (+5%)	79.19	+0.23%
H_u=5.0 mm	4.75 mm (–5%)	78.21	+0.02%
H_l =10.0 mm	10.5 mm (+5%)	78.23	+0.05%
H_l =10.0 mm	9.5 mm (–5%)	78.40	+0.26%
NACA4609	NACA 3609 (m–1)	74.72	–4.44%
NACA4609	NACA 5609 (m+1)	76.81	–1.77%
NACA4609	NACA 4509 (p–1)	75.55	–3.37%
NACA4609	NACA 4709 (p+1)	76.26	–2.47%
NACA4609	NACA 4608 (ta–1)	76.65	–1.98%
NACA4609	NACA 4610 (ta+1)	75.08	–3.98%

From a sensitivity analysis for the design variables as was mentioned in section 4, the resulting changes in volume flow rate of air are listed in Table 2. Based on Table 2 it is obvious that by giving the same scale of perturbation for each variable, the corresponding changes are prominent for only the m, p, ta, θ, Lr and Le six variables. This implies that these six variables are sensitive to the volume flow rate of air, and therefore they are chosen as the key design variables in the present study, i.e. the design variables used for the present blade shape design problem are now taken as follows:

$$\mathbf{B} = \{B_1, B_2, B_3, B_4, B_5, B_6\} = \{\, m, p, ta, \theta, Lr, Le \,\}. \quad (25)$$

The rest of the system parameters are kept constant in the entire calculation. With the above six design variables the following fan blade design problem can be performed

In the optimal fan blade design problem, a very large number for desired volume flow rate of air Θ at Ps equal to zero is assigned and the Levenberg-Marquardt method is utilized to obtain the optimal shape of fan blade that meets the requirement as close as possible. The objective function cannot reduce to a small number in this case, but the optimal shape for fan blade can still be obtained.

By requiring 20% increase in the volume flow rate of air at Ps = 0, i.e., setting Θ = 93.8 CFM at Ps = 0, and using the system variables for the original fan blade as the initial guesses for the design variables. After six iterations, the design variables for m, p, ta, θ, Lr and Le can be obtained and are listed in Table 1. From there it can be learned that the volume flow rate of air for the optimal fan blade is only 88.84 CFM at Ps = 0, i.e., the airflow rate is increased by 13.6% only, which implies that the increase of 20% airflow rate cannot be reached, but still the best increase in airflow rate can be obtained. Fig. 2(b) shows the comparison of the blade shape for original and optimal fans.

Next, it is of interest to examine that if the required airflow rate is less than 88.84 CFM, can the design algorithm obtain such a fan blade that meets the requirement exactly. First, it is required that Θ = 63 CFM at Ps = 0, (i.e., less than the airflow rate for the original fan), then it is increased to Θ = 83 CFM at Ps = 0.

The design variables for the above two specified design problems can be obtained by utilizing LMM; after 5 and 6 iterations, respectively, the design variables can be obtained and are listed in Table 1. From Table 1 it is clear that for the designed fan blade #1, the airflow rate is calculated as Q = 63 CFM at Ps = 0, and for the designed fan blade #2, the airflow rate is calculated as Q = 83 CFM at Ps = 0. They are identical to the desired airflow rates, Θ = 63 CFM and Θ = 83 CFM, respectively. This implies that the present design can design the fan blade with specified airflow rate; of course, it must be less than the optimal airflow rate.

The numerical solutions for original and optimal fans in Ps–Q and η–Q curves are shown in Figs. 3 and 4, respectively. It can be seen from these two figures that the optimal fan performs better than the original fan since it has higher airflow rate under same static pressure and higher fan efficiency under same airflow rate.

As was mentioned previously, the statistical analysis is important in determining the reliability of the estimated design variables. For this reason the 99% confidence bounds for the estimated variables must be calculated. For the optimal fan the airflow rate is obtained as 0.042 m^3/s; assuming that the stan-

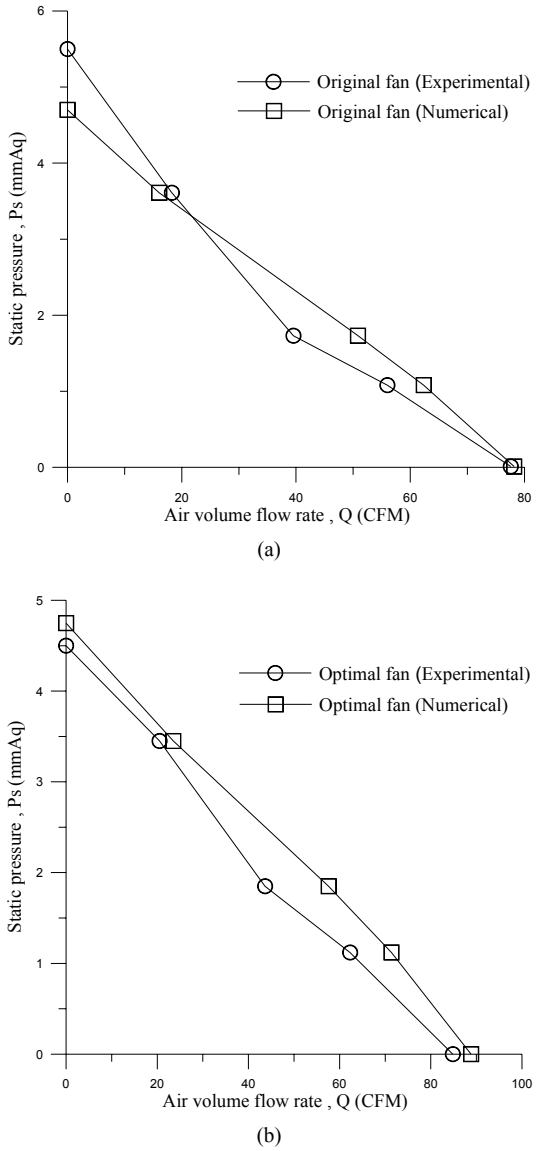

Fig. 3. Comparisons of the numerical and experimental results in Ps–Q curve for (a) original; (b) optimal fan blades.

dard deviation of the airflow measurement is 10% error of the airflow rate, this means $\sigma = 0.0042$ can be used to calculate the standard deviation of design variables as well as the 99% confidence bounds.

The calculated results for the standard deviation of design variables and the 99% confidence bounds are shown in Table 3. It can be seen that with 10% measurement error in airflow rate, the estimated standard deviation of design variables is very small, and thus the band of the 99% confidence bounds becomes very narrow. This implies that the present design algorithm is reliable since most of the design is within these narrow bounds.

The accuracy of the solution from CFD code in flow field calculations for fans plays an important role in this fan blade design problem. If the solution from CFD code cannot reproduce the actual performance of the fan blades, the design can never be obtained accurately. The first task is thus to show the validity of the solutions from CFD code by comparing them with the experimental data. The benchmark problems for the numerical solution in airflow rate of fans using CFD code must be examined here based on the experiments conducted in this work for the original and optimal fan blades.

Table 3. The estimated standard deviation and 99% confidence bounces for the design variables in optimal fan blade with $\sigma = 0.0042$.

	θ	Lr	Le	m	p	ta
σ_B	0.00008	0.00019	0.00008	0.00021	0.00025	0.00012
$B_{mean}-2.576\sigma_B$	58.9997	19.3795	37.8597	4.9995	5.9993	7.9997
B_{mean}	59.0	19.38	37.86	5	6	8
$B_{mean}+2.576\sigma_B$	59.0002	19.3805	37.8602	5.0005	6.0006	8.0003

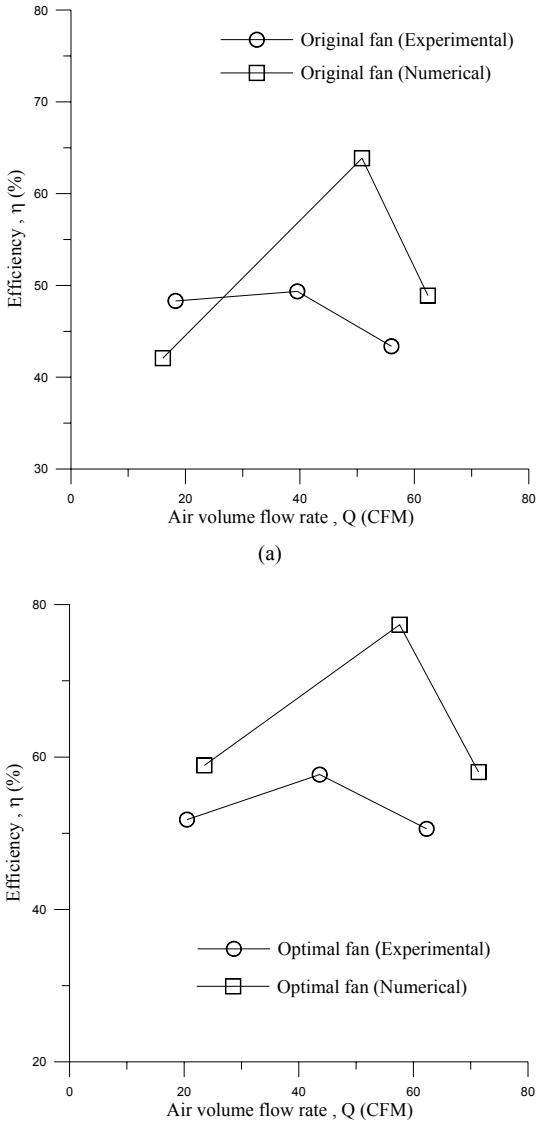

Fig. 4. Comparisons of the numerical and experimental results in η–Q curve for (a) original; (b) optimal fan blades.

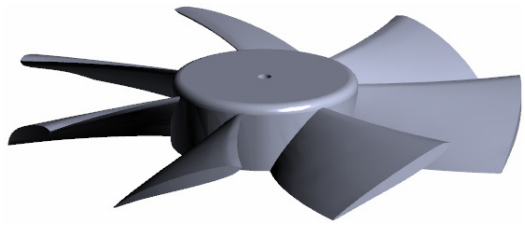

(a)

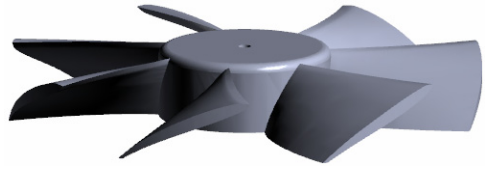

(b)

Fig. 5. The solid shapes for (a) original; (b) optimal fan blades.

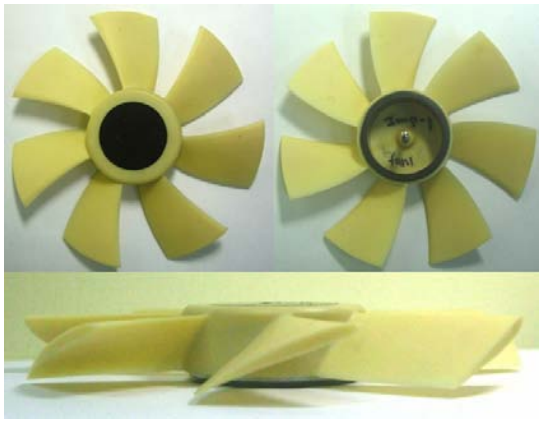

(a)

(b)

Fig. 6. The CNC machine fabricated (a) original and (b) optimal fan blades.

For this reason the original and optimal fan blades must be CNC fabricated in accordance with our design. Figs. 5(a) and 5(b) indicate the solid shapes for the original and optimal fan blades that were obtained from our numerical data. The numerical data can be used in the CNC machine to fabricate fan blades

(a)

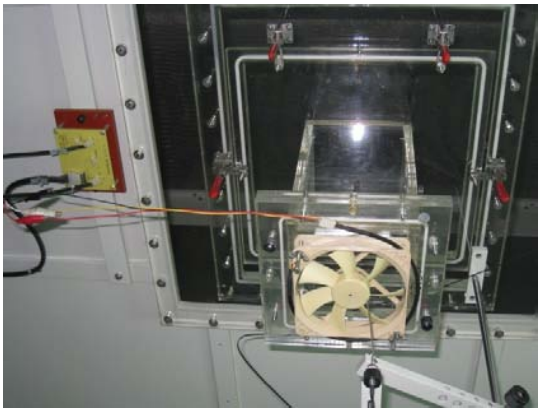

(b)

Fig. 7. The experimental apparatus for the (a) entire fan test section; (b) fan blade test section.

in reality that can be used in experiments. Figs. 6(a) and 6(b) show the fabricated original and optimal fan blades, respectively.

The experimental apparatus for entire fan test section and fan blade test section is given in Figs. 7(a) and 7(b), respectively, and the operational conditions for fan blades testing have been described in the preceding section. Figs. 8(a) and 8(b) indicate the experimental results for Ps–Q and rpm–Q curves for original and optimal fan blades, respectively. From Fig. 8 it can be learned that the experiments performed quite well since the fan speed keeps almost constant at ω = 2500 rpm for all the different testing cases considered here. The trend of the Ps-Q curve for both fan blades is also reasonable.

The experimental results for original and optimal fans in Ps–Q and η–Q curves are also shown in Figs. 3 and 4, respectively. It can be seen from Fig. 3 that at the design point (Ps = 0), the airflow rates for original and optimal fan blades are obtained as 77.595 CFM and 84.842 CFM, respectively. This implies a 9.34% increase in the airflow rate. Although in numerical simulations there is a 13.6% increase in the airflow rate for optimal fan blade, but still the design is effective since 9.34% increase in the airflow rate is quite a significant number. However, at higher static pressure, the original fan blade has better performance in airflow rate. This may be due to some

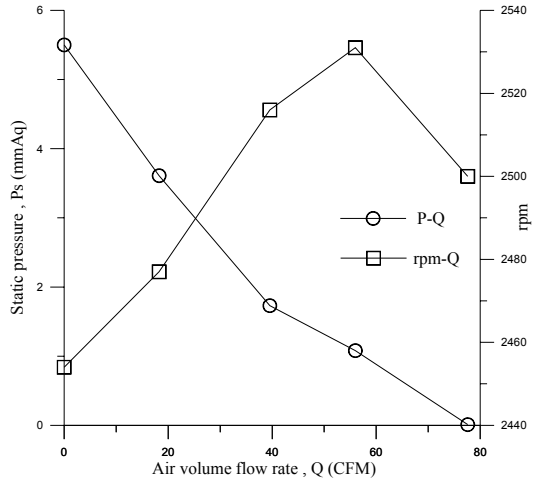

Fig. 8. The experimental results for Ps–Q and rpm–Q curves in (a) original; (b) optimal fan blades.

errors induced in the experiment measurements, but from Fig. 4 it is clear that fan efficiency for the optimal fan blade is always higher than that for the original fan. From Figs. 3 and 4 we have obtained the evidence that the designed optimal fan blade indeed has better performance than the original fan blade.

The final task is to compare the numerical results with the experimental results for both the original and optimal fans. The purpose of this check is to verify the accuracy of the above numerical optimal design for fan blades. Figs. 3(a) and 3(b) show the comparisons of the numerical and experimental results in Ps–Q curve for the original and optimal fan blades, respectively. At the design point, Ps = 0, the numerical and experimental airflow rates are obtained as 78.19 CFM and 77.59 CFM for original fan blade, respectively, i.e., the error is only 0.77%, while for optimal fan blade, they are obtained as 88.84 CFM and 84.84 CFM, respectively, and the error is also only 4.7%. The maximum error between the numerical and experimental airflow rates is calculated as 25.3% for the original fan and is 29.5% for the optimal fan.

There always exists a discrepancy between experimental measurements and numerical simulation for any engineering problems. It may be due to either simulation error or experimental error or both. In the present study the error at the design condition, Ps = 0, is very small, 0.77%, for the original fan and 4.7% for the optimal fan, but for the other operation conditions, larger error can be obtained but that is still acceptable for engineering applications. From the above results it can be concluded that the present numerical solutions for fan blade design problems are reliable and the design of blades can be used in reality.

The comparisons of the numerical and experimental results in η–Q curve for original and optimal fan blades are shown in Figs. 4(a) and 4(b), respectively. It is obvious from Fig. 4(b) that the efficiency calculated by the numerical method is higher than that for the experimental result except for one position for the original fan blade at low airflow rate. This may be due to the experimental error performed in fan testing.

10. Conclusions

A fan blade design problem in estimating the optimal shape of a fan blade for an axial-flow fan based on the knowledge of desired volume flow rate of air, commercial CFD code and Levenberg-Marquardt method has been examined successfully in this study. Numerical calculations are performed first to design the optimal shapes of fan blades; experiments are conducted then to verify the accuracy and validation of the estimations. Results show that the present algorithm needs only a few iterations to obtain the optimal shapes of fan blades, and the volume flow rate of air and fan efficiency can both be increased by using the estimated fan blades.

The advantages of using the present technique in designing the optimal shape of fan blades lie in the fact that (1) the time needed to redesigning the shape of blade can be shortened, and (2) the desired airflow rate can be well matched, when compared with the traditional trial and error method.

Acknowledgment

This work was supported in part through the National Science Council, R. O. C., Grant number, NSC-100-2221-E-006-011-MY3.

Nomenclature

B_j : Design variables
$E(\bullet)$: The expected value
H_l : Lower hub height
H_u : Upper hub height
J : Functional defined by Eq. (5)
Le : Blade end chord
Lr : Blade root chord
m : Blade section parameter
Ps : Static pressure

Q : Calculated airflow rate
ta : Blade section parameter
$\bar{u}_i$: Flow velocity

Greeks

$\mathfrak{J}$: Jacobian matrix defined by Eq. (14)
Ψ : Fan blade domain
μ^n : Damping parameter
η : Fan efficiency
ω : Fan speed
ϕ : Twist angle
θ : Setting angle
Θ : Desired airflow rate
τ : Torque of fan blade
σ : Standard deviation

References

[1] S. Kalpakjian and S. R. Schmid, *Manufacturing processes for engineering materials*, Second Ed. Addison-Wesley, New York, USA (1992).
[2] B. Eck, Fans design and operation of centrifugal, Axial-Flow, and Cross-Flow Fans, Oxford Pergamon Press, New York, USA (1973).
[3] R. A. Wallis, Axial flow fans and ducts, A Wiley- Interscience Publication, USA (1983).
[4] M. Zangeneh, Inviscid-viscous interaction method for 3d inverse design of centrifugal impellers, *ASME Journal of Turbomachinery,* 116 (1994) 280-290.
[5] A. Demeulenaere and R. Van den Braembussche, Three-dimensional inverse method for turbomachinery blading design, *ASME Journal of Turbomachinery,* 120 (1998) 247-255.
[6] J. S. Kim and W. G. Park, Optimized inverse design method for pump impeller, *Mechanics Research Communications,* 27 (4) (2000) 465-473.
[7] B. J. Lin, C. I. Hung and E. J. Tang, An optimal design of axial-flow fan blades by the machining method and an artificial neural network, *Proc. Instn. Mech. Engrs. Part C: J Mechanical Engineering Science*, 216 (2002) 367-376.
[8] S. J. Seo, S. M. Choi and K. Y. Kim, Design optimization of a low-speed fan blade with sweep and lean, *Proc. IMechE Part A: J. Power and Energy*, 222 (2008) 87-92.
[9] K. S. Lee, K. Y. Kim and A. Samad, Design optimization of low-speed axial flow fan blade with three-dimensional rans analysis, *Journal of Mechanical Science and Technology*, 22 (2008) 1864-1869.
[10] K. Y. Lee, Y. S. Choi, Y. L. Kim and J. H. Yun, Design of axial fan using inverse design method, *Journal of Mechanical Science and Technology*, 22 (2008) 1883-1888.
[11] CFD-RC user's manual, ESI-CFD Inc. (2005).
[12] J. S. Arora, Introduction to optimum design, McGraw-Hill, New York (1989).
[13] D. M. Marquardt, An algorithm for least-squares estima tion of nonlinear parameters, *J. Soc. Indust. Appl. Math.*, 11 (1963) 431-441.
[14] C. H. Huang, C. C. Chiang and S. K. Chou, An inverse geometry design problem in optimizing the hull surfaces, *Journal of Ship Research*, 42 (1998) 79-85.
[15] P. F. Chen and C. H. Huang, An inverse hull design approach in minimizing the ship wave, *Ocean Engineering*, 31 (2004) 1683-1712.
[16] P. F. Chen, C. H. Huang, M. C. Fang and J. H. Chou, An inverse design approach in determining the optimal shape of bulbous bow with experimental verification, *Journal of Ship Research*, 50 (2006) 1-14.
[17] C. H. Huang, L. Y. Chen and S. Kim, An inverse geometry design problem in optimizing the shape of gas channel for proton exchange membrane fuel cell, *J. Power Sources*, 187 (2009) 136-147.
[18] C. H. Huang and J. W. Lin, Optimal gas channel shape design for a serpentine pemfc--theoretical and experimental studies, *J. Electrochemical Society*, 156 (2009) B178-B187.
[19] Y. T. Yang and H. S. Peng, Numerical study of pin-fin heat sink with un-uniform fin height Design, *International Journal of Heat and Mass Transfer*, 51 (2008) 4788-4796.
[20] Y. T. Yang and H. S. Peng, Numerical study of the heat sink with un-uniform fin width designs, *International Journal of Heat and Mass Transfer*, 52 (2009) 3473-3480.
[21] R. W. Farebrother, Linear least square computations. marcel dekker, Inc., New York (1988).
[22] A. M. Maniatty and N. J. Zabaras, Investigation of regularization parameters and error estimating in inverse elasticity problems, *Int. J. Numer. Methods Engineering*, 37 (1994) 1039-1052.
[23] G. P. Flach and M. N. Ozisik, Inverse heat conduction problem of simultaneously estimating spatially varying thermal conductivity and heat capacity per unit volume, *Numerical Heat Transfer*, 16 (1989) 249-266.

Cheng-Hung Huang received his B.Sc. degree form National Cheng Kung University, Tainan, Taiwan, in 1983, and M.Sc. and Ph.D degrees from the North Carolina State University, Raleigh, NC, USA, in 1991, all in the Mechanical Engineering department. In 1991, he joined the faculty of the Department of Systems and Naval Mechatronic Engineering, National Cheng Kung University, Tainan, Taiwan, where he is currently a professor. His research interests include inverse problems, system design problems and system identification problems.

Chung-Wei Gau received his B.Sc. degree from National Chung Hsing University in Bio-Industrial Mechatronics Engineering and M.S. from National Cheng Kung University in Systems and Naval Mechatronic Engineering department, in 2008 and 2010, respectively.